Characterization of the count rate performance of modern gamma cameras

M. Silosky
Department of Imaging Physics, The University of Texas MD Anderson Cancer Center, Houston, Texas 77030 and Graduate School of Biomedical Sciences, The University of Texas Health Science Center, Houston, Texas 77030

V. Johnson
Quantitative Sciences Division, The University of Texas MD Anderson Cancer Center, Houston, Texas 77030

C. Beasley
Department of Diagnostic and Interventional Imaging, The University of Texas Medical School, Houston, Texas 77030

S. Cheenu Kappadath[a)]
Department of Imaging Physics, The University of Texas MD Anderson Cancer Center, Houston, Texas 77030 and Graduate School of Biomedical Sciences, The University of Texas Health Science Center, Houston, Texas 77030

(Received 12 October 2012; revised 31 January 2013; accepted for publication 31 January 2013; published 27 February 2013)

Purpose: Evaluation of count rate performance (CRP) is an integral component of gamma camera quality assurance and system deadtime (τ) may be utilized for image correction in quantitative studies. This work characterizes the CRP of three modern gamma cameras and estimates τ using two established methods (decay and dual source) under a variety of experimental conditions.
Methods: For the decay method, uncollimated detectors were exposed to a Tc-99m source of relatively high activity and count rates were sampled regularly over 48 h. Input count rate at each time point was based on the lowest observed count rate data point. The input count rate was plotted against the observed count rate and fit via least-squares to the paralyzable detector model (PDM) to estimate τ (rates method). A novel expression for observed counts as a function of measurement time interval was derived, taking into account the PDM and the presence of background but making no assumption regarding input count rate. The observed counts were fit via least-squares to this novel expression to estimate τ (counts method). Correlation and Bland-Altman analyses were performed to assess agreement in estimates of τ between the rates and counts methods. The dependence of τ on energy window definition and incident energy spectrum were characterized. The dual source method was also used to estimate τ and its agreement with estimates from the decay method under identical conditions was also investigated. The dependences of τ on the total activity and the ratio of source activities were characterized.
Results: The observed CRP curves for each gamma camera agreed with the PDM at low count rates but deviated substantially from it at high count rates. The estimates of τ determined from the paralyzable portion of the CPR curve using the rates method and the counts method were found to be highly correlated ($r = 0.999$) but with a small ($\sim$6%) difference. No statistically significant difference was observed between the estimates of τ using the decay or dual source methods under identical experimental conditions ($p = 0.13$). Estimates of τ increased as a power-law function with decreasing ratio of counts in the photopeak to the total counts. Also, estimates of τ increased linearly as spectral effective energy decreased. No significant difference was observed between the dependences of τ on energy window definition or incident spectrum between the decay and dual source methods. Estimates of τ using the dual source method varied as a quadratic on the ratio of the single source to combined source activities and linearly with total activity.
Conclusions: The CRP curves for three modern gamma camera models have been characterized, demonstrating unexpected behavior that necessitates the determination of both τ and maximum count rate to fully characterize the CRP curve. τ was estimated under a variety of experimental conditions, based on which guidelines for the performance of CRP testing in a clinical setting have been proposed.
 [http://dx.doi.org/10.1118/1.4792297]

Key words: deadtime, gamma camera, quality assurance, decay method, dual-source method

I. INTRODUCTION

I.A. Current status

Evaluation of count rate performance (CRP) is an integral component of routine quality assurance testing for gamma cameras. Additionally, the American College of Radiology (ACR) requires that count rate performance be evaluated at least annually as part of a nuclear medicine accreditation program.[1] While the National Electrical Manufacturers Association has provided procedure guidelines for CRP testing (decay method),[2] the suggested procedure requires at least 48 h of acquisition time, making it cumbersome to perform routinely in a clinical setting. An alternative method for evaluating CRP, commonly referred to as the dual source method, has been suggested by Adams *et al.*[3] AAPM Report No. 6 echoes this recommendation, suggesting that system deadtime be evaluated using the dual source method under specific conditions of scatter and count rates.[4] While performance of the dual source method is convenient due to short acquisition times (10–15 min), it is valid only for systems that have been demonstrated to follow the paralyzable detector model (PDM). Historically, gamma cameras have been assumed to follow the PDM, and several earlier generation gamma cameras were explicitly demonstrated to be paralyzable.[3] In recent years, advances in hardware and new methods of signal processing have resulted in improved CRP. With recent improvements in technology, it remains to be demonstrated that the PDM is appropriate for modern gamma cameras.

In addition to the need for an appropriate method of CRP evaluation required as a part of routine quality assurance, an investigation of the CRP of modern gamma cameras can provide the means of obtaining an important parameter, the system deadtime (τ). As the interest in quantitative SPECT continues to grow, the ability to provide corrections for count rate losses may become important. While count rates typically observed during diagnostic nuclear medicine imaging procedures rarely approach those that result in significant losses, imaging procedures performed after internal radionuclide therapies have been observed to result in high count rates ($\sim$250 kcps in an open energy window) and consequently lead to substantial count rates losses.[5] In many cases, imaging post internal radionuclide therapy is intentionally delayed or even not performed due to concerns over count rate losses. The ability to correct for count rate losses in post radionuclide therapy imaging may be necessary to quantitatively validate the delivery of the prescribed amount of radionuclide to the target in cases where saturation of binding cites may occur (e.g., radioimmunotherapy).[6] To accurately perform these corrections, a thorough understanding of the CRP and system deadtime of modern gamma cameras, including its dependence on the incident energy spectrum and energy window selected, is required.

The objectives of this investigation are (1) to determine whether the CRP curves for several modern gamma cameras follow the PDM, (2) to determine under what conditions estimates of τ determined using the dual source method, agree with those determined using the decay method, and (3) to provide guidelines regarding the estimation of τ using these methods. To achieve these objectives, CRP was evaluated for three modern gamma camera models from different manufacturers using both the decay (Secs. II.A and III.A) and dual source (Secs. II.B and III.B) methods, under a variety of different experimental conditions (Secs. II.C and III.C). Furthermore, data from the decay method were analyzed using two different techniques; namely, the rates method (Sec. II.A.1) and the counts method (Sec. II.A.2).

I.B. Paralyzable detector model

In the PDM, the observed count rate (m) of a counting system may be related to the input count rate (n) by the following equation:[7]

$$m = ne^{-(n\tau)}, \tag{1}$$

where τ represents the system deadtime. Additionally, it has been demonstrated that τ for a paralyzable detector is related to the maximum observed count rate (MCR) through the following equation:[3]

$$\tau = \frac{1}{e \times \mathrm{MCR}}. \tag{2}$$

As a result of this relationship, a single parameter, either τ or MCR, may be used to describe the CRP of an ideal paralyzable detector.

I.C. CRP evaluation: Decay method

The decay method for evaluating CRP consists of exposing an uncollimated detector to a radioactive source (typically Tc-99m) and sampling the count rate at intervals over a period of time sufficient such that radioactive decay results in low observed count rates where losses are negligible. For a paralyzable detector, initial activity is selected such that the input count rate is greater than what is required to reach MCR. Background measurements are performed before and after this acquisition and used to correct the observed count rates. On the basis of the assumption that count rate losses are negligible at low count rates, the background corrected lowest count rates measured are considered to be equivalent to the input count rate. The input count rates corresponding to all other observed count rates are subsequently estimated by scaling the lowest count rate by the relative decay in activity due to the difference in time in accordance with the following equation:[2]

$$n_i = m_n e^{\lambda(t_n - t_i)}, \tag{3}$$

where n_i represents the input count rate for data point i, m_n is lowest background corrected observed count rate, λ is the decay constant of the radioactive source, and t_i and t_n are the relative times at which measurements for data points i and n were performed, respectively. Two important points should be noted in regards to this procedure. First, count rate losses are assumed to be negligible for the measurements of the background and the lowest observed count rates. Second, low count rate data points are particularly sensitive to the magnitude of the background corrections.

With the input count rate and observed count rate determined for each data point, the CRP curve can be plotted to determine the MCR. For an ideal paralyzable detector, τ may be calculated from this MCR using Eq. (2). In practice, it has been demonstrated that even for gamma cameras that have been primarily characterized as paralyzable, τ estimated from MCR can vary substantially.[8] The advantage of the decay method is that the entire CRP curve, including MCR (the most common metric quoted by vendors), is directly measured. The disadvantage is that the decay method requires data acquisition over long intervals ($\sim$ 2 days) while maintaining a relatively constant background and curve fitting software will be needed to determine τ.

I.D. CRP evaluation: Dual source method

The dual source method for evaluating CRP involves making count rate measurements using two sources of similar activity, with the detector exposed to each source individually and then concurrently. As with the decay method, these measurements must be corrected for background. Once these measurements are made, τ may be estimated based on the following equation:[3]

$$\tau = \frac{2R_{12}}{(R_1 + R_2)^2} \ln\left(\frac{R_1 + R_2}{R_{12}}\right), \tag{4}$$

where R_1 and R_2 are the background corrected observed count rates for sources 1 and 2, respectively, and R_{12} is the background corrected observed count rate for sources 1 and 2 concurrently. Equation (4) may be derived directly from Eq. (1) with the assumption that sources 1 and 2 are equal in activity and result in similar observed count rates. The advantage of the dual source method is that τ may be estimated algebraically, with data acquisition occurring over a relatively short interval (<10 min), and without the use of curve fitting software. The disadvantages are that the gamma camera in question must follow the PDM for Eq. (4) to be valid and that MCR is not directly measured.

II. MATERIALS AND METHODS

II.A. Characterization of CRP using the decay method

To characterize the CRP of modern gamma cameras, the decay method was performed to measure the CRP curve on several Symbia (Siemens Medical Systems, Malvern, PA), a Brightview (Philips Medical Systems, Andover, MA), and a Millennium MG (General Electric Healthcare, Waukesha, WI) gamma cameras. The uncollimated detectors were exposed to a Tc-99m source positioned at approximately 5 FOV and counts were acquired for sequential counting intervals over a 48-h period. No additional edge shielding was used, since these systems have rectangular gamma camera detectors which often have a built-in mask to prevent edge-packing. The initial source activities ranged between 111 and 370 MBq (3 and 10 mCi) depending on the camera tested and distance to the detector. For the Symbia and Brightview cameras, counting intervals were 2 min for the first 12 h, followed by 4, 8, and 16-min intervals for 12 h periods each, for a total of 675 measurements. For the Millennium MG, the first two 12-h periods were composed of 2- and 4-min intervals, respectively, followed by 24 h of 16-min intervals, for a total of 630 measurements. The Symbia was evaluated with the source placed in a syringe free-in-air (AIR) and using an open energy window (OW) intended to capture counts across the entire spectrum. The OW was composed of the following adjacent energy windows: 17.5–52.5, 52.5–157.5, 157.5–472.5, and 472.5–687.3 keV. Additionally, the Symbia was evaluated with the source placed in a cylindrical lead shield with an open end covered by 6 mm of copper plates (NEMA) and using the manufacturer's recommended 15% photopeak window in accordance with NEMA NU1-2007 recommendations for performing the decay method.[2] The Brightview was evaluated using the AIR scatter condition and an OW. The Millennium was evaluated using the NEMA scatter condition and the manufacturers recommended 20% photopeak window. Background measurements of 10 min were performed prior to and after the decay method data acquisition. The resulting data for each detector were evaluated using two methods; rates and counts (described next), to identify the portion of the CRP curve that followed the PDM and to estimate the value of τ associated with this portion.

II.A.1. Rates method procedure

The rates method for evaluating decay method measurement data involves fitting the observed and input count rates to the PDM [Eq. (1)] via nonlinear least-squares regression. The observed count rates were determined for each data point and the input count rates were estimated based on Eq. (3), but modified to account for the effects of interframe decay resulting from different counting interval durations as follows:[7]

$$n_i = m_n e^{\lambda(t_n - t_i)} \times \frac{\Delta t_n (1 - e^{-\lambda \Delta t_i})}{\Delta t_i (1 - e^{-\lambda \Delta t_n})}, \tag{5}$$

where Δt_n and Δt_i are the durations of counting intervals n and i, respectively. To evaluate the quality of the least-squares fit, the root mean square (RMS) of the residuals (fit-measurement) was calculated. Visual inspection of CRP data (Fig. 1) indicated that only a portion of the CRP curve followed the PDM. To identify the input count rate at which the CRP curve begins to deviate from the PDM, the fit was repeated with data points removed sequentially from the high count rate end of the curve. A threshold of less than 2% for RMS residuals was chosen to establish that the CRP data range was adequately described by the PDM. Additionally, the percentage change in RMS residuals was calculated for each fit when consecutive data points were removed. Small changes in RMS residuals imply that the fit converged and consequently the model parameter does not change substantially, i.e., the value of τ, determined from the fit is relatively stable. With this rationale, τ in this work was determined from the fit of measured CRP data at the value where the RMS residuals were below 2% and where RMS residuals changed by less than 1% from the previous fit (which included one additional CRP measurement).

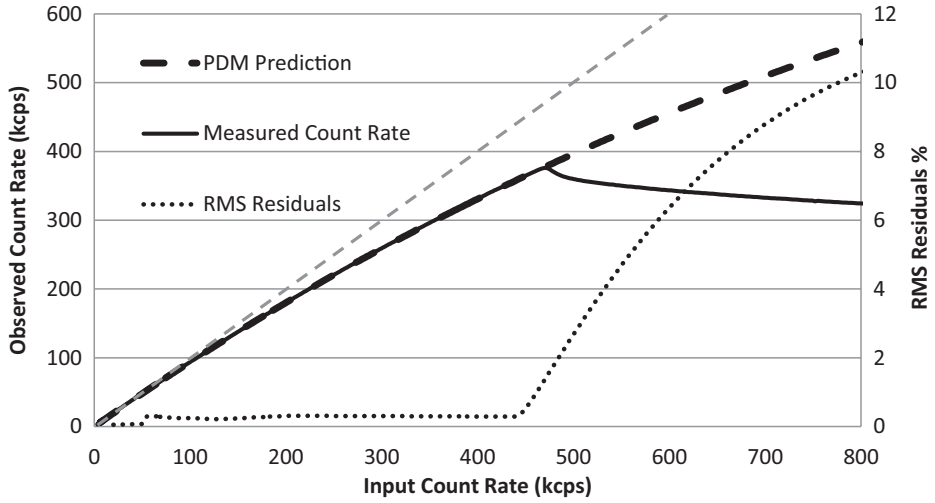

FIG. 1. The measured CRP curve for a typical Symbia detector acquired using a Tc-99m source (AIR) and an open energy window is plotted along with the ideal CRP behavior predicted by the PDM. For this detector, the observed CRP appears to agree well with the PDM prediction up to a certain observed count rate (~375 kcps), beyond which the observed count rate deviates dramatically. The RMS residuals calculated for least-squares fits of the observed count rates up to a maximum input count rate to the PDM (rates method) are shown plotted against the maximum input count rate included in the fit. The quality of the fit improves and RMS residuals decreases as the maximum input count rate included in the fit decreases. When the fitted observed count rate data range lies along the paralyzable portion of the CRP curve, the RMS residuals cease to decrease and the quality of the fit remain relatively constant. The gray dashed line represents the line of identity.

Although the rates method is a relatively straight-forward procedure for determining τ for decay method data, the two important points previously discussed (in Sec. I.C) with regards to this procedure were addressed. First, care was taken to ensure that low count rates (<4 kcps) were observed for the last count rate measurement. Second, the decay method data collections were performed under quiescent and stable background conditions.

II.A.2. Counts method procedure

To further address the concerns mentioned above, we have developed a new procedure (counts method) for analyzing decay method data that does not base an estimate of input count rates on a single data point. A novel expression was derived from the PDM for the counts observed during a counting interval from t_0 to t_1, assuming the background count rate was subject to count rate losses and the input count rate was subject to radioactive decay. In this case, the input count rate, n can be expressed as

$$n(t) = b + A_0 e^{-\lambda(t-t_0)}, \tag{6}$$

where b is the background count rate, A_0 is the portion of the input count rate due entirely to the decay of the source at time t_0, λ is the decay constant for the source in question, and t is the time since t_0.

Substituting Eq. (6) for n in Eq. (1) and integrating over a time interval from t_0 to t_1 results in the following expression for the counts observed during that interval, $M(t_0,t_1)$, that accounts for losses due to the background

$$M_{(t_0,t_1)} = be^{-b\tau}\int_{t_0}^{t_1} e^{-(A_0 e^{-\lambda t})\tau}dt + \frac{e^{-b\tau}}{\lambda\tau}(e^{-(A_0\tau e^{-\lambda t_1})} - e^{-(A_0\tau e^{-\lambda t_0})}). \tag{7}$$

As shown in the Appendix, the solution to Eq. (7) can be written as

$$M_{(t_0,t_1)} = \frac{e^{-b\tau}}{\lambda\tau}(e^{-(A_0\tau e^{-\lambda t_1})} - e^{-(A_0\tau e^{-\lambda t_0})}) + be^{-b\tau}(t_1 - t_0) + \frac{A_0\tau}{\lambda}be^{-b\tau}(e^{-\lambda t_1} - e^{-\lambda t_0})\left(1 - \frac{A_0\tau}{2}e^{-\frac{\lambda(t_1+t_0)}{2}} + \frac{(A_0\tau)^2}{6}e^{-\lambda(t_1+t_0)} - \frac{(A_0\tau)^3}{24}e^{-\frac{3\lambda(t_1+t_0)}{2}}\right). \tag{8}$$

The counts measured over known time intervals (Fig. 2) using the decay method can be modeled using Eq. (8) to estimate τ, b, and A_0. The "data interval index" shown in Fig. 2 refers to a scalar value (starting from 1) assigned for each measurement interval during data acquisition with the decay method. No background measurements or estimates of input count rate are required for this method. The counts method was used to fit the decay data, and the RMS residuals were calculated. This fit and RMS calculation were repeated as data points were removed for the high count rate end of the CRP curve. The percentage change in RMS residuals from the previous data point was calculated (Fig. 2). As with the rates method, a threshold of less than 2% for RMS residuals was chosen to indicate that the fitted CRP data were adequately described by the PDM and the model parameters (τ, b, and A_0) were determined at the data point where RMS residuals changed by less than 1% from the previous fit.

II.A.3. Precision in estimates of τ

To evaluate the precision in τ estimated using both the rates and counts methods, decay measurements were performed five times on the same, dual-headed 3/8 in. crystal, Symbia system using the AIR scatter condition and OW. The

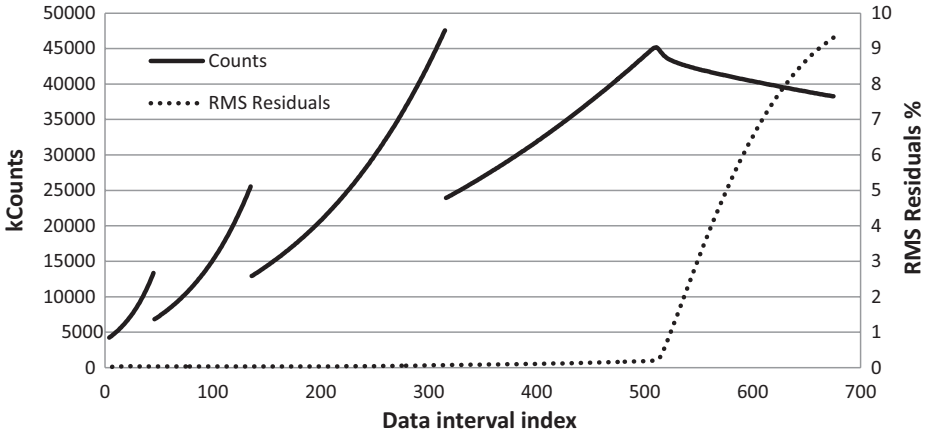

FIG. 2. The observed counts at each counting interval plotted against the "data interval index" for a Symbia 3/8 in. crystal detector. The data interval index refers to a scalar value assigned to each of the measurement intervals for data acquisition with the decay method. Because the decay data start with measurements performed at high activity, the first measurement at the highest input count rate corresponds to index value 675 and the last measurement with the lowest input count rate corresponds to index value 1. Discontinuities in the observed counts (at index values of 45, 135, and 316) are the result of doubling the counting interval duration every 12 h to help maintain uniform counting statistics. The observed discontinuity at the index value of 508 is due to the deviation of the measured count rate from the PDM. The RMS residuals calculated for least-squares fits of the observed counts to the PDM (counts method) are shown plotted against the maximum data interval included in the fit. Similar to the rates method, as high count rate data points are removed from the fit, its quality improves and the RMS residuals decreases. When the fitted observed count data lie along the paralyzable portion of the CRP curve, the RMS residuals cease to decrease and the fit quality remains relatively constant.

mean value of τ (τ_m), standard deviation (σ), and fractional error in τ were calculated where

$$\text{Fractional error}\,(\%) = (\sigma/\tau_m) \times 100. \tag{9}$$

II.A.4. Assessment of agreement between rates and counts methods

To assess agreement between the rates and counts methods, τ was determined for 42 decay method data sets performed using various gamma cameras, energy windows, and spectral conditions using both methods. The mean difference, the standard error in the mean difference, and the standard deviation of the differences were calculated. A paired t-test was performed to evaluate the magnitude and significance of the difference. The degree of correlation between the two methods was evaluated by calculating the Pearson product-moment correlation coefficient (r). Additionally, a Bland-Altman analysis[9] was performed to characterize correlation between methods and to evaluate for potential biases.

II.B. Estimation of τ using the dual source method

Dual source measurements were performed on a number of different Symbia gamma camera detectors without collimators (intrinsic acquisition) with sources placed at approximately 5 FOV from the detectors. No additional edge shielding was used for any dual source measurements. The procedure began with a 30-s background measurement. Next, measurements were made for five consecutive counting intervals, each of 5-s duration with the detectors exposed to source 1. These five measurements were repeated with the detectors exposed to both sources, and then repeated again with the detectors exposed only to source 2. Another 30-s background measurement was performed. Because the collimators were removed, sources with activities between 55.5 and 74 MBq (1.5–2.0 mCi) resulted in count rates that approached the MCR for these systems, allowing the counting intervals to be kept short while still obtaining a reasonable number of counts. Because of the high input count rates (intrinsic data acquisition), even short acquisition times, as low as 5 s, yielded high count floods (in millions of counts) preserving good counting statistics. Five independent values for R_1, R_2, and R_{12} were determined by dividing the counts in each interval by its duration and subtracting the mean background count rate. Time between the first measurement of source 1 and last measurement of source 2 was kept short ($\Delta t < 1.5$ min) to minimize the effects of radioactive decay (during the measurement source activity varied by less than 0.5%).

II.B.1. Source activity ratio dependence

To evaluate the dependence of τ, estimated using the dual source method, on the inequality of source activities, the dual source method was performed as described in Sec. II.B on two Symbia detectors using an open energy window and two In-111 sources. In-111 was chosen because its relatively long half-life compared to the duration of the experiment, mitigating the effects of radioactive decay. Initial source activities were chosen such that source 1 contained approximately 90% of the total activity and source 2 contained approximately 10%. Five independent sets of dual source measurements were performed. Following these measurements, a fraction of the activity in source 1 was transferred to source 2 and the measurements were repeated. This process was repeated until the relative activities of sources 1 and 2 were approximately

reversed, resulting in nine activity ratios. For each combination, the activities of sources 1 and 2 were measured in a dose calibrator and the ratio of the activity of source 1 to the total activity was determined. For each activity ratio used in the dual source method, the mean value of τ was calculated. The range of τ, given the range of activity ratios used, was determined. The functional form of the dependence of τ on the ratio of activity of source 1 to the total activity was determined. The ratio of the activities of source 1 to the total activity that result in changes of 1% and 5% in τ when compared to an estimate of τ using sources of equal activity were determined.

II.B.2. Count rate dependence

To evaluate the dependence of τ estimated using the dual source method on count rate, the dual source method was performed on two Symbia detectors using two Tc-99m sources, an open energy window, and the AIR spectral condition. Activities were selected such that R_{12} was less than 5% of the MCR. Five independent sets of dual source measurements were performed. Following data acquisition, the activity for both sources was increased and the measurements were repeated. This procedure was repeated until the combined activities of sources 1 and 2 provided an input count rate beyond MCR. The activities for sources 1 and 2 were always maintained to be within 2% of each other. The mean value of τ was calculated at each level of total activity. A range of count rates where the estimates of τ were relatively stable was identified. The functional form of the dependence of τ on total activity was determined for the stable range.

II.B.3. Precision

To evaluate the precision in estimates of τ, the dual source method was performed for two Siemens Symbia detectors using Tc-99m, an open energy window, the AIR spectral condition, and a total activity selected such that R_{12} was ~95% of MCR. The activities for sources 1 and 2 were within 2% of each other. Five trials were performed, resulting in five separate measurements of R_1, R_2, and R_{12}. Because each of these measurements is independent, 125 permutations of R_1, R_2, and R_{12} are possible. τ was estimated for all 125 permutations of R_1, R_2, and R_{12} using Eq. (4). The mean value of τ, standard deviation, and fractional error were calculated.

II.C. Effect of energy window definition and incident spectrum on estimates of τ

II.C.1. Energy window definition

To evaluate the effect of energy window definition on estimates of τ, both the decay and dual source methods were performed five times on a dual-headed, 3/8 in. crystal, Symbia system, using different photopeak window widths of 2%, 6%, 15%, 75%, and an OW using Tc-99m and the AIR scatter condition. Collimators were removed and no additional edge shielding was used. A spectrum was acquired on each detector with sufficient source activity such that the observed count rate was approximately 95% of MCR (roughly 125.8 MBq or 3.4 mCi). τ was estimated for the paralyzable portion of the CRP curves for all detectors using both the rates and counts methods. Additionally, source activities for the dual source method were maintained within 2% of each other, and the total activity was selected such that the R_{12} was ~95% of MCR (roughly 62.9 MBq or 1.7 mCi per source). The total activity varied by less than 5% between energy windows. The energy spectrum was used to calculate the ratio of counts in each photopeak window, to the total counts. The functional form of the dependence of τ on the ratio of photopeak window to total counts was determined for both the decay data using the rates method and the dual source method. An estimate of τ, for a 20% photopeak window was performed and the difference between the 15% and 20% windows was calculated.

To determine if there is a statistically significant difference in the dependence of τ on the ratio of photopeak window to total counts between the decay (rates) and dual source methods, values of τ and the ratios were made linear by taking the natural logarithm. These "linearized" values were fit using linear least squares regression and the 95% confidence intervals were determined for the slopes and intercepts.

II.C.2. Incident spectrum dependence

To evaluate the effects of incident energy spectrum on estimates of τ, two Symbia detectors were evaluated using the decay and dual source methods with an OW under a series of different scatter conditions. Collimators were removed and no additional edge shielding was used. In addition to the AIR and NEMA recommended scatter conditions, the following three conditions were used to acquired data with the decay method: a source placed in an acrylic scatter block (20 × 20 × 15 cm, recommended for CRP testing in AAPM Report No. 6) placed at 5 FOV from the detector (SCATTER), a source placed in the same acrylic scatter block describe above with 8.4 cm of acrylic (7 sheets, 1.2 × 23 × 23 cm) placed between block and detector, and a source placed in the acrylic scatter block with a small lead shield (approximately 0.2 cm thick) inserted next to the syringe, positioned between the source and the detector to attenuate radiation emitted in the direction of the detector but allow radiation scattered from the sides and rear of the block to interact with the detector, resulting in the relative reduction of the photopeak. Source activity was varied between 126 and 740 MBq (3.4–20 mCi) depending on the amount of scattering material used. Data were analyzed using both the rates and counts methods. The dual source method was performed for two Siemens detectors using seven different spectral conditions. These conditions were modified through a combination of radionuclides (Tc-99m, In-111, or Tl-201) and the use of acrylic scattering material, and lead shields with copper filters as described for the AIR, SCATTER, and NEMA setups. The measurements were performed twice with In-111, once using the AIR setup, and once using the NEMA setup with individual source activities of 44.4 and 185 MBq (1.2 and 5.0 mCi), respectively. The measurements were performed three times with Tc-99m,

using the AIR, SCATTER, and NEMA setups with individual source activities of 62.9, 59.2, and 227.6 MBq (1.7, 1.6, and 6.15 mCi), respectively. The measurements were performed twice with Tl-201, using the AIR and SCATTER setups with individual source activities of 62.9 and 66.6 MBq (1.7 and 1.8 mCi), respectively. Five trials were performed for each spectral condition. For each scatter condition, a spectrum was acquired on both detectors at or near MCR. The effective energy of each spectrum was calculated by summing the products of the counts in each energy bin by its assigned energy, and then dividing it by the total counts acquired across the entire spectrum. The functional form of the dependence of τ on effective energy was determined for decay method using both rates and counts and the dual source method. The range in τ, for the different effective energies used, was determined. Additionally, the change in effective energy that resulted in a 5% change in τ was calculated.

To determine if there is a statistically significant difference between the dependence of τ on effective energy, values of τ and the effective energies for both methods were fit using linear least squares regression. The 95% confidence intervals were determined for both the slopes and intercepts.

II.D. Assessment of agreement between decay (rates) and dual source methods

τ was determined for 25 combinations of gamma camera detector, energy windows, and spectral conditions using both the decay (rates) and dual source methods. The mean difference, the standard error of the mean difference, and the standard deviation of the differences were calculated. A paired *t*-test was performed to evaluate the significance of the mean difference. The degree of correlation between the two methods was evaluated by calculating the Pearson product moment correlation coefficient (r). Additionally, a Bland-Altman analysis was performed to characterize correlation between methods and to evaluate potential biases.

III. RESULTS

III.A. Characterization of CRP using the decay method

III.A.1. CRP curves and PDM fit results

The CRP curves for all three cameras tested were visually observed to agree with the PDM at low count rates. However, as input count rates increased, each system eventually reached a point where its behavior substantially deviated from the PDM (Fig. 3). The MCR that was observed for each of these systems occurred below the MCR predicted by the PDM. Lowest count rate data point measurements were performed at approximately 4 kcps. Based on estimates of τ (Table I), losses due to deadtime at this count rate were low (<0.5%).

Table I shows the fitted estimates of τ and MCR using both the rates and counts. Also shown are the measured MCR and the corresponding value of τ for an ideal paralyzable detector. Additionally, the measured background rate (b) and initial input count rates (A_0) estimated with the rates method were found to be in good agreement with the fitted values of b and A_0 (free parameters) using the counts method. Values of A_0 differed by 3% and the background rates differed by 1 kcps or less between the two methods. Also, the observed count rates at which the detectors reached the 2% RMS residual criteria (see Sec. II.A) are listed. These values differ by approximately 1% or less between the two methods.

III.A.2. Precision in estimates of τ

Repeat measurements performed on the Symbia system using a Tc-99m source, OW, and the AIR spectral condition, resulted in mean ± standard deviation values of

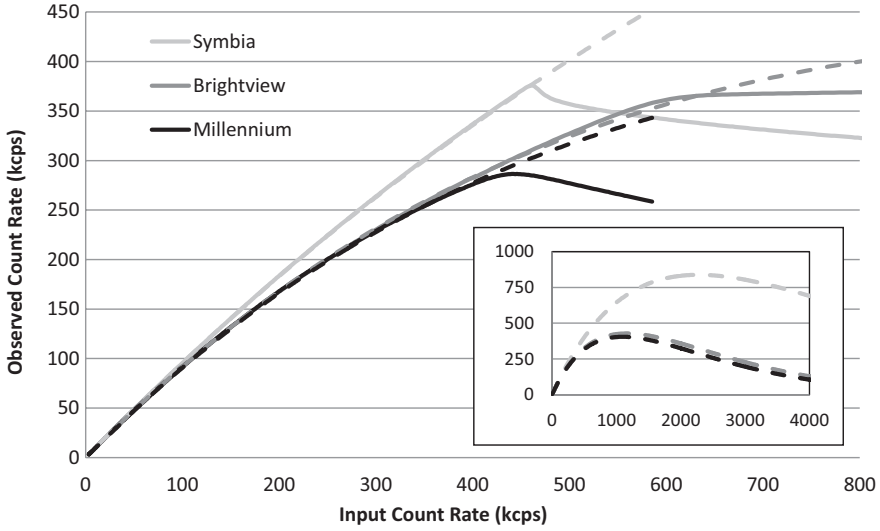

FIG. 3. The observed CRP curves for three modern gamma cameras (solid lines) are plotted along with the ideal CRP behavior predicted by the PDM (dashed lines). As higher input count rates are approached, all three gamma cameras have a distinct cutoff beyond which the system no longer follows the PDM. Relative to the Symbia, the Brightview and Millennium deviated more gradually from the PDM. The inset shows the behavior predicted by the PDM for these detectors at higher input count rates. The observed count rates increases with the input count rates, reaches a maximum, and then decreases. Unlike the observed behavior, the rollover at MCR for an ideal paralyzable detector occurs smoothly with no discontinuities and related to the deadtime τ.

TABLE I. Deadtime, τ for the paralyzable portion of the CRP curve determined using both the rates and counts methods are tabulated with background count rate, initial input count rate, and the observed count rate where RMS residuals are less than 2% for both detectors of three different gamma cameras. Additionally, the MCR predicted from estimates of τ, observed MCR, and τ predicted from MCR using the PDM are tabulated to illustrate the differences between modern gamma camera performance and PDM predictions.

Camera	τ (μs)	τ predicted from MCR (μs)	MCR (kcps)	MCR predicted from τ (kcps)	Background rate (kcps)	Initial input rate (kcps)	Observed rate @ 2% RMS residual (kcps)
				Rates Method			
Symbia	0.439	0.978	376	838	0.626	869	354
Symbia	0.405	1.013	363	908	0.617	853	341
Brightview	0.859	0.927	397	428	1.419	6388	369
Brightview	0.857	0.951	387	429	1.352	5181	362
Millennium	0.909	1.286	286	405	0.232	620	277
Millennium	0.956	1.251	294	385	0.195	597	335
				Counts Method			
Symbia	0.410	0.978	376	897	0.552	862	355
Symbia	0.376	1.013	363	979	0.541	846	342
Brightview	0.837	0.927	397	440	2.428	6197	370
Brightview	0.967	0.951	387	380	1.220	5187	365
Millennium	0.900	1.286	286	408	−0.023	618	280
Millennium	0.906	1.251	294	406	0.106	611	333

0.441 ± 0.00342 μs and 0.407 ± 0.00256 μs for detectors 1 and 2, respectively, using the rates method. The counts method resulted in mean $\pm$ standard deviation values of 0.413 $\pm$ 0.00324 μs and 0.377 ± 0.00121 μs for detectors 1 and 2, respectively. In all cases, the fractional error in estimates of τ was less than 1%.

III.A.3. Assessment of agreement between rates and counts methods

A high degree of correlation was observed for the estimates of τ between the rates and counts methods ($r = 0.999$, $p < 0.001$) using data from 42 decay method data sets acquired under various combinations of detector, spectral conditions, and energy window. Figure 4 shows the Bland-Altman plot for the estimate of τ using the two methods with the mean estimate as the abscissa and their difference as the ordinate. The mean and standard deviation of the differences in τ between the two methods were calculated to be 0.029 and 0.050 μs, respectively. The differences in τ roughly followed a normal distribution and, more importantly, did not vary with the average estimate for τ. The mean difference could be interpreted as an estimate of the bias in τ between the two methods. With a standard error in the mean difference of 0.008 μs, the 95% confidence interval for the bias between the two methods was calculated to be 0.013 and 0.044 μs. The bias was found to be statistically significant ($p < 0.05$ for two-tailed t-test) but small in magnitude (0.029 μs).

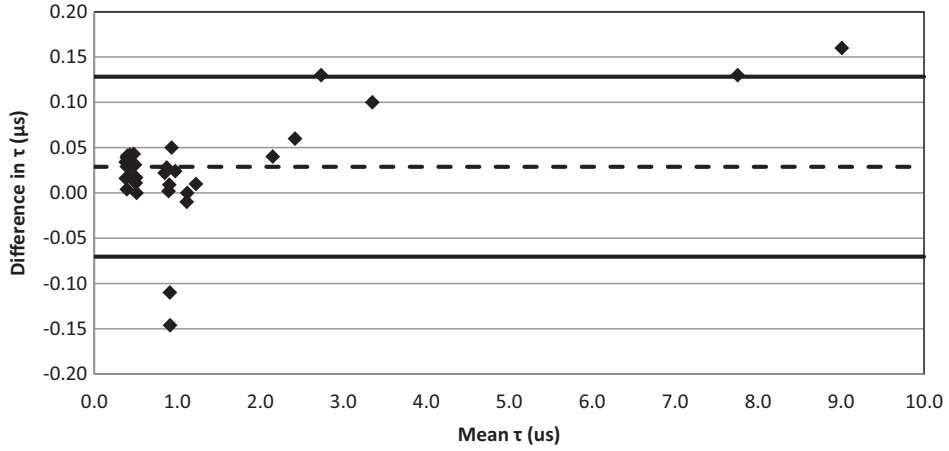

FIG. 4. A Bland-Altman plot of agreement for τ calculated using the rates and counts methods. The difference in τ for the two estimates (ordinate) is plotted against their mean values (abscissa). The data plotted include 42 decay method data sets acquired under various combinations of detector, spectral conditions, and energy window. The dashed line represents the mean difference in τ ($\Delta\tau = 0.029$ μs), and the solid lines represent $\pm$ 2 standard deviations ($\sigma = 0.050$ μs).

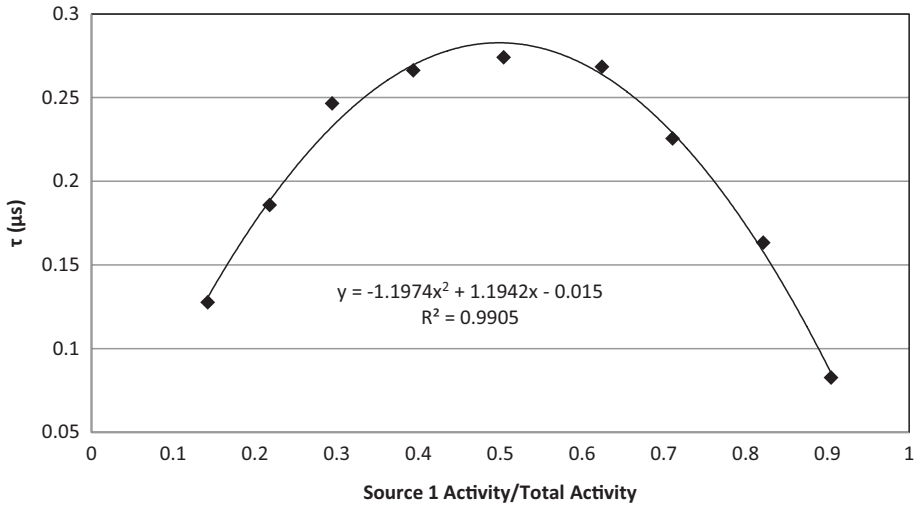

FIG. 5. The plot of τ estimated using the dual source method (using In-111) for a Symbia 3/8 in. detector as a function of the ratio of source 1 activity to the total activity (source 1 + source 2). The data could be modeled as a quadratic function with a maximum value of τ occurring at a ratio of single source activity to total activity of 0.50.

III.B. Estimation of τ using the dual source method

III.B.1. Source ratio dependence

The observed dependence of estimates of τ on the ratio of the single source activity to the total activity (Fig. 5) could be modeled as a quadratic function. Estimates of τ varied by about 300%, from 0.083 μs with single source 1 at 90.4% of the total activity to 0.274 μs with single source 1 at 50.4% of the total activity. Based on the quadratic fit, estimates of τ performed using the dual source method were within 5% of the maximum value when the ratio of single source to total activity was maintained between 39% and 61%, and τ was within 1% of the maximum value when the ratio of single source to total activity was maintained between 44% and 55%.

III.B.2. Count rate dependence

Dual source method estimates of τ varied substantially with the total activity used (Fig. 6). Three distinct regions of behavior were observed. At lower activities where R_{12} was less than about 35% MCR, estimates of τ decreased rapidly and were subject to large fluctuations. For activities selected such that R_{12} was greater than 35% MCR but still within the paralyzable portion of the CRP curve, estimates of τ had a slowly varying linear dependence. At activities that result in count rates beyond the paralyzable portion of the CRP curve, values of τ again increased rapidly. Within the relatively stable region where R_{12} was between 35% and 95% MCR, estimates of τ ranged from 0.372 to 0.430 μs

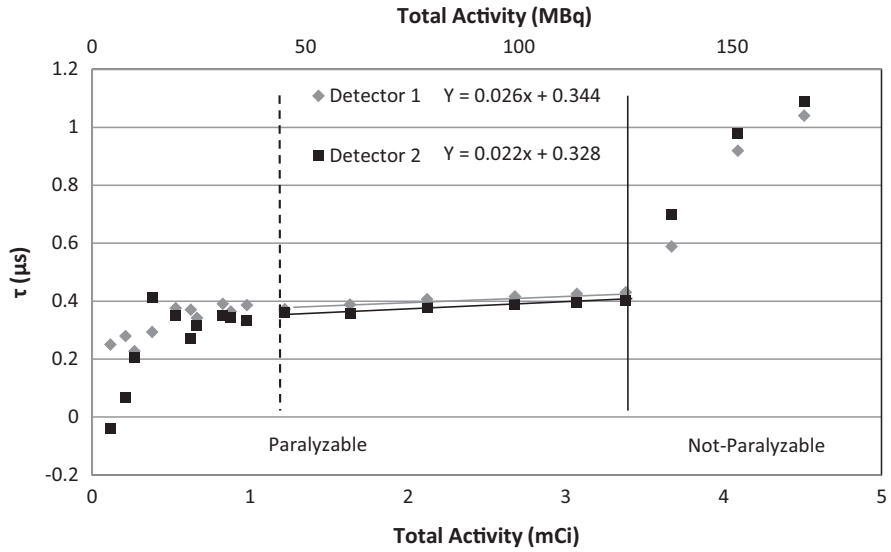

FIG. 6. The plot of τ estimated using the dual source method (Tc-99m) for two Symbia 3/8 in. detectors plotted as a function of the total activity used. The stable region is indicated by the two vertical lines. The upper bound is indicated by the solid vertical line that corresponds to the activity at which ~95% MCR is observed. The lower bound is indicated by the dashed line that corresponds to the activity at which ~35% MCR is observed. When performing the dual source method, activities should be selected such that the total activity falls within the relatively stable region, preferably near the high count rate or activity region.

($\Delta\tau = 14.5\%$) for detector 1 and 0.360 to 0.402 μs ($\Delta\tau = 11.0\%$) for detector 2.

III.B.3. Precision

The mean ± standard deviation values of τ for the 125 permutations of the R_1, R_2, and R_{12} for detectors 1 and 2 were 0.430 ± 0.002 and 0.407 ± 0.004 μs, respectively. For both detectors, the fractional error was less than 1%, similar to the precision of the decay method.

III.C. Effect of energy window definition and incident spectrum on estimates of τ

III.C.1. Energy window definition

Energy window definition was observed to have a substantial effect on both decay and dual source method estimates of τ. Estimates of τ ranged from 0.441 μs for an OW to 7.82 μs for the 2% photopeak window for detector 1 and from 0.407 μs for an OW to 9.09 μs for the 2% photopeak window for detector 2 using the decay method. Using the dual source method, estimates of τ ranged from 0.434 μs for an OW to 8.20 μs for the 2% photopeak window for detector 1 and from 0.406 μs for an open energy window to 11.17 μs for the 2% photopeak window for detector 2. For both methods, this change in τ is approximately 2000%. τ was shown to be related to the ratio of photopeak window counts to total counts by a power law function, as shown in Figs. 7(a) and 7(b). The ratios of counts in the photopeak window to the total counts were approximately 46.1% and 50.4% for the 15% and 20% photopeak windows, respectively, resulting in estimates of τ that differed by 12.45% for the decay method and by 12.75% for the dual source method.

As seen in Figs. 8(a) and 8(b), a linear relationship is observed when the natural logarithm of τ is plotted against the natural logarithm of the ratio of the photopeak window to the total counts. The linear fit for both the decay (rates) and dual source methods fell within the 95% confidence interval of each other for both detectors, indicating that there is no statistically significant difference between the relationships observed using these two methods.

III.C.2. Incident spectrum dependence

As the effective energy of the incident spectrum increased, the estimates of τ were observed to decrease linearly for both the decay and dual source methods. Figures 9(a) and 9(b) show the linear fits for each detector using both methods and the corresponding 95% confidence intervals. Estimates of τ using the decay method varied 17% and 19% in the energy range from 99.1 to 143 keV for detectors 1 and 2, respectively. Estimates of τ using the dual source method varied 43.4% and 42.5% in the energy range from 87.3 to 181.6 keV for detectors 1 and 2, respectively. Also, a 5% change in the value of τ resulted from a change in effective energy of 11.8 and 10.6 keV for detectors 1 and 2 using the decay method, and 10.4 and 9.3 keV for the same using the dual source method. The linear fits for both the decay and dual source methods fall within the 95% confidence intervals of each other for both detectors, indicating that there is no statistically significant difference between the relationships observed using these two methods.

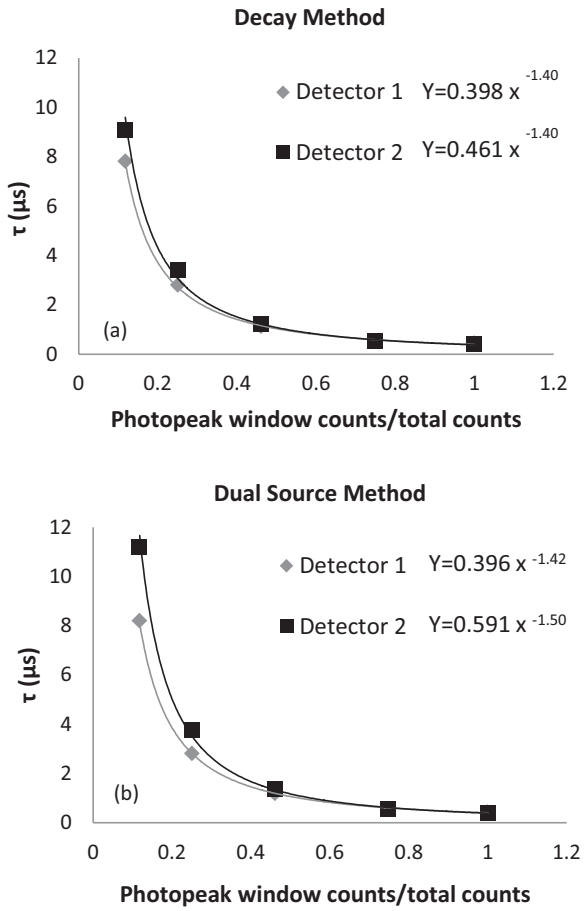

FIG. 7. The estimates of τ plotted against the ratio of counts in the photopeak window to total counts in the spectrum (OW) for two Symbia 3/8 in. detectors using the decay method (a) and the dual source method (b) for two Symbia 3/8 in. detectors.

III.D. Assessment of agreement between decay (rates) and dual source methods

A high degree of correlation was observed for the estimates of τ between the decay and dual source methods ($r = 0.996$, $p < 0.001$) using data from 25 pairs of measurements utilizing various detectors, spectral conditions, and energy windows. Figure 10 shows the Bland-Altman plot for the estimate of τ using the two methods with the mean estimate as the abscissa and their difference as the ordinate. The mean and standard deviation of the differences in τ between the two methods were calculated to be −0.131 and 0.420 μs, respectively. The differences in τ roughly followed a normal distribution and, more importantly, did not vary with the average estimate for τ. The mean difference could be interpreted as an estimate of the bias in τ between the two methods. With a standard error in the mean difference of 0.084 μs, the 95% confidence interval for the bias between the two methods was calculated to be −0.304 and 0.042 μs. The bias was found to be statistically not significant ($p = 0.13$ for two-tailed t-test).

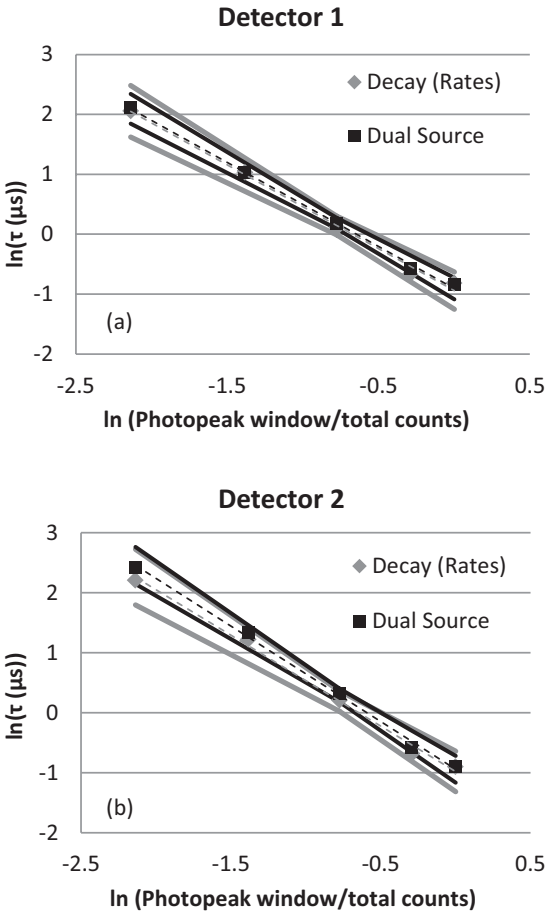

FIG. 8. The natural logarithm of τ plotted against the natural logarithm of the ratio of counts in the photopeak window to the total counts for two Symbia 3/8 in. detectors (a) and (b). The dashed lines represent the least-squares fits to linear functions and the solid lines represent the 95% confidence intervals for these fits.

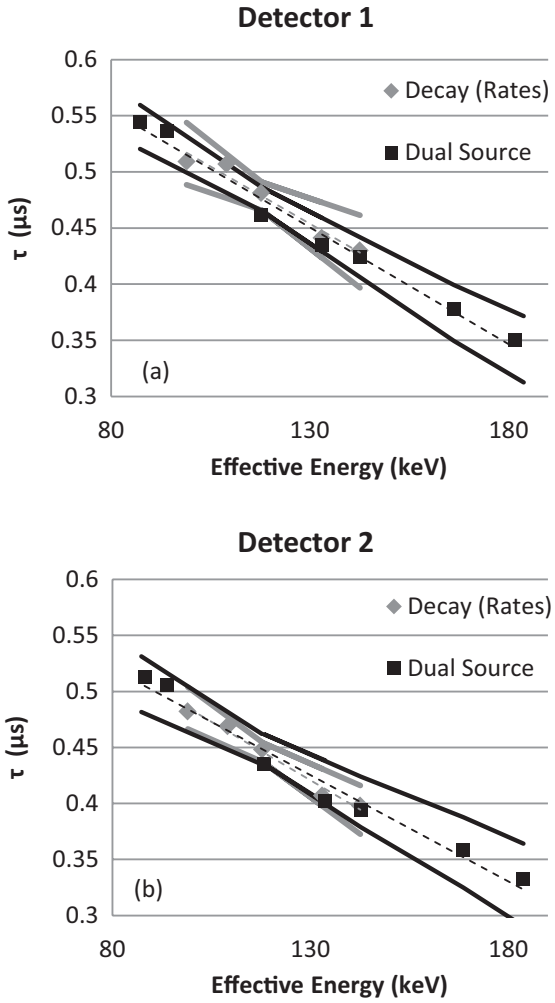

FIG. 9. The estimates of τ plotted against the effective energy of the incident spectrum using the decay and dual source methods for two Symbia 3/8 in. detectors (a) and (b). The dashed lines represent the least-squares fit to linear functions and the solid lines represent the 95% confidence intervals for these fits.

IV. DISCUSSION

IV.A. CRP of modern gamma cameras

It has been observed that the CRP curves of the three modern gamma camera models investigated do not follow the PDM at all count rates. However, good agreement with the PDM was observed up to reasonably high input count rates (300–400 kcps, OW), beyond which these systems deviated substantially from the PDM. Owing to this behavior, the observed MCR for these cameras fell well below the predicted MCR assuming the PDM. As a result, MCR can no longer be directly related to τ via Eq. (2), indicating that it may not provide an adequate metric for evaluating CRP. Since routine clinical imaging is always performed in the paralyzable portion of the CRP curve, τ, estimated for this portion of the curve, is a better indicator of clinical CRP.

IV.B. Comparison of rates and counts methods for analyzing decay method data

While it was observed that estimates of τ determined using the rates method and the counts method were highly correlated, a small but significant bias was detected. Because the true values of τ for these gamma cameras are not known, there is no strong justification to claim that one method provides a more accurate estimate than the other. Estimates of the input count rate and the background used in the rates method were found to be consistent with the predicted values from the counts method (Table I), suggesting that the assumption of minimal losses at low count rates (<4 kcps) used to estimate input count rate and correction for the background in the rates method was reasonable. Because the counts method does not base estimates of input count rate on the lowest count rate data point it may be possible to reduce the total time required for the data acquisition; conferring on it a practical advantage over the rates method.

IV.C. Specific concerns regarding dual source method performance

To ensure reliable quality control, it is important to perform the dual source method using consistent energy windows and spectral conditions. It was observed that if the ratio

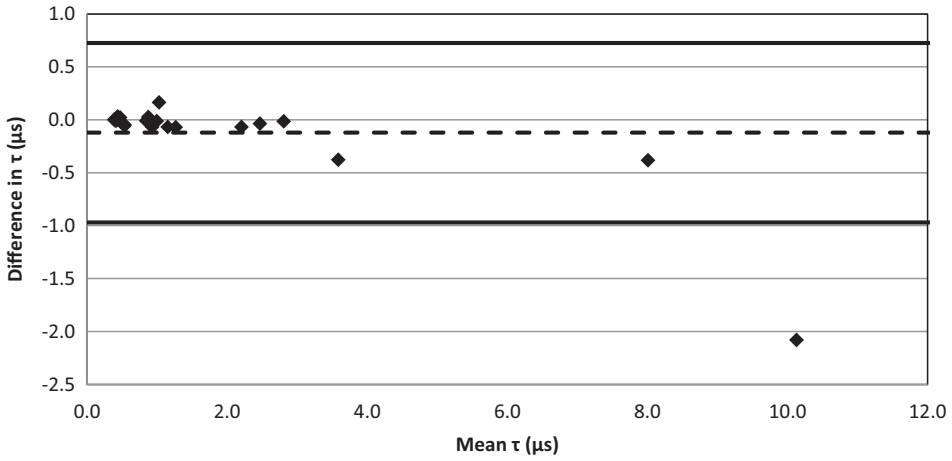

FIG. 10. A Bland-Altman plot of agreement for τ calculated using both the decay (rates) and dual source methods. The mean value of the two estimates (ordinate) is plotted against their difference (abscissa). The data plotted include 25 pairs of measurements using various detectors, spectral conditions, and energy windows The dashed line represents the mean difference in τ ($\Delta\tau = -0.131$ μs) and the solid lines represent ± 2 standard deviations ($\sigma = 0.419$ μs).

of the individual source activity to the total activity is maintained between 40% and 60%, τ can be expected to be within 5% of its value when the sources are of exactly equal activity. If sources are maintained between 45% and 55%, this can be reduced to ~1%. Also, the count rate dependence of estimates of τ using the dual source method requires that the total activity be consistent and that R_{12} falls within the paralyzable portion of the CRP curve (from about 35% to 95% of MCR for a Siemens Symbia). It should be noted that the observed count rate dependence (Fig. 6) is specific to the gamma camera it was tested on (Siemens Symbia). Adams *et al.*[3] observed that this dependence varied significantly between several earlier generation models. Given these observations, dual source measurements intended to estimate τ should be performed with an activity such that R_{12} is near the highest count rate that falls within the paralyzable portion of the CRP curve.

IV.D. Comparison of decay and dual source methods for evaluating CRP

The estimates of τ determined using the decay method and the dual source method were found to be highly correlated with no statistically significant difference between them when R_{12} is maintained at about 95% of MCR. Because τ is an appropriate metric for evaluating CRP, the dual source method can be used for routine quality control. Given the convenience with which the dual source method can be performed and its excellent agreement with the results of the decay method, the dual source method is ideal for obtaining estimates of τ for the paralyzable portion of the CRP curve. For both methods, estimates of τ may vary greatly with the ratio of counts in the energy window to the total counts. Effective energy has a smaller but not insignificant effect on estimates of τ with the difference between the AIR and NEMA scatter conditions less than 5% when using an OW. Therefore, it is imperative to use consistent energy windows and scatter conditions when performing CRP testing to evaluate changes in performance.

IV.E. Comparison and comments on manufacturer specification

This work has demonstrated that a direct comparison to the manufacturer's specifications requires identical energy window and spectral conditions during CRP measurement. For the Symbia, Brightview, and Millenium MG gamma cameras, the manufacturer has provided the MCR as a performance specification observed (310, 350, and 220 kcps, respectively) in accordance with NEMA recommendations. Both the Symbia and Millenium cameras were evaluated under similar conditions resulting in MCR observed at 240 and 294 kcps, respectively. A separate evaluation of Symbia deadtime using the dual source method (AAPM Report No. 6) yielded τ values of 1.424 and 1.374 μs for 3/8 and 5/8 in. crystals, respectively.[10] In addition, variations in the incident spectrum and consequently the ratio of the photopeak window counts to the total counts, can have a substantial effect on the observed counts. Therefore, a direct comparison of MCR or τ with other experiments or manufacturer's specifications is challenging. While the observed count rate at 20% loss has been provided by some manufacturers, its value as a performance specification may be limited because it has been observed that some modern cameras deviate from the paralyzable model prior to 20% loss occurring. Moreover, calculation of the count rate at any arbitrary percentage loss can be performed once τ has been determined for the system.

For the purposes of acceptance testing, it may be beneficial for the manufacturers to provide specifications performed in a manner such that variation in the experimental setup does not lead to large fluctuations in the result. To address this issue, performance metrics (either MCR or τ) may be evaluated using an OW. It has been shown that the effects of spectral variations are mitigated when counts are observed across the entire spectrum. Additionally, since the MCR observed for the modern cameras tested cannot be directly related to count rate losses, MCR has become less valuable as a performance metric. As a result, τ estimated for the paralyzable portion of the CRP curve using an OW and the maximum paralyzable count

rate may be more appropriate metrics for comparison to manufacturers specifications. On the basis of these observations, we suggest that manufacturers consider including an open energy window selection.

IV.F. Guidelines for acceptance and annual CRP testing

Because the CRP varies between different gamma camera models, it is our recommendation that CRP be evaluated using the decay method during acceptance testing of a new camera to determine τ, MCR, and the corresponding input count rate and source activity at which MCR occurs. Placing the source or sources at 5 FOV from an uncollimated detector is a common testing geometry and a source holder can be easily constructed to maintain reproducibility. Additionally, an energy window should be selected for data acquisition. While theoretically an OW would be ideal for this purpose assuming that it was used by the manufacturer to determine performance specifications, the photopeak window defined by the manufacturer for Tc-99m (15% or 20%) is acceptable for this purpose. At this time, a reproducible testing geometry, energy window, and scatter conditions should be identified and all further tests should be performed in the same manner. Care should be taken to ensure low and stable background conditions during data acquisition. If the decay data are to be analyzed via the rates method, then the last measurement with low source activity should be acquired at low count rates and a final background measurement should be performed after the source has been removed. Following decay method acquisition, the data may be analyzed using either the rates or counts methods to determine both τ for the paralyzable portion of the CRP curve and the maximum count rate at which the system agrees with the PDM. Additionally, the dual source method should be performed utilizing the same geometry, scatter conditions, and energy windows as the decay method (sources placed at 5 FOV, uncollimated detectors, and no additional scattering material). The total activity should be selected such that it results in count rates near (90%–95%) MCR but within the paralyzable region of the CRP curve. Owing to the relatively high count rates used, acquisition times may be kept short and correction for radioactive decay may be ignored. A background measurement, followed by measurements of source 1 only, sources 1 and 2, source 2 only, and a second background should be performed. Estimates of τ may be obtained through the use of Eq. (4). Future evaluations of CRP (e.g., annual testing) may be performed using the dual source method alone ensuring consistent use of testing geometry, scatter conditions, energy windows, and activities.

IV.G. Corrections for count rate loss and quantitative imaging

Imaging following internal radionuclide therapy could result in appreciably high input count rates, where the ability to correct for count rate losses would be necessary to quantitatively ascertain the delivery of the prescribed activity of radionuclide to the target. Although count rates losses during typical diagnostic imaging procedures may be relatively low, correction for count rate losses may still be necessary for quantitative SPECT and planar imaging. This work has reported on various strategies that could be used for estimation of the system deadtime of gamma cameras. Additionally, the results presented in this work of describing the functional relationships of the estimates of τ on the incident energy spectrum and on the energy windows may be useful in developing a procedure for the correction for these losses.

V. CONCLUSION

The CRP curves for three modern gamma camera models have been characterized demonstrating unexpected behavior. Agreement with the PDM was observed only at low count rates with a marked deviation from PDM at high input count rates. The mathematical relationship between τ and MCR [Eq. (2)] has been shown to be no longer valid, necessitating the determination of both τ and MCR to fully characterize the CRP curve. A novel method to analyze decay data using the measured counts (counts method) was presented and shown to be consistent with, if not superior to, the conventional rates method. A detailed analysis of correlation between the estimates of τ using the decay and the dual source methods showed no statistically significant differences. The estimates of τ were shown to depend on the ratio of counts in the photopeak window to the total counts as a power law function and linearly with the effective energy of the input spectrum. The estimates of τ using the dual source method were observed to vary as a quadratic on the ratio of the single source to combined source activities and linearly with total activity used. On the basis of these investigations, guidelines for the performance of CRP testing in a clinical setting have been provided.

APPENDIX: DERIVATION OF EXPRESSION REPRESENTING MEAN COUNTS OBSERVED DURING A COUNTING INTERVAL FROM T_0 TO T_1, ACCOUNTING FOR SOURCE DECAY

For a paralyzable detector exposed to a decaying radioactive source, the mean observed count rate (m) may be related to the mean input count rate (n) via the following expression:

$$m = ne^{-n\tau}, \tag{A1}$$

where τ represents the system deadtime. The mean input count rate is a function of both the background count rate (b) and the decay of the source and can be represented with the following equation:

$$n(t) = b + A_0 e^{-\lambda t}, \tag{A2}$$

where λ is the decay constant of the source, t is time, and A_0 is the input count rate at $t = 0$. The mean counts observed during a counting interval from t_0 to t_1 ($M_{(t_0,t_1)}$) may be determined by substituting Eq. (A2) into Eq. (A1) and integrating the mean observed count rate over the time interval in question as

$$M_{(t_1,t_0)} = \int_{t_0}^{t_1} (b + A_0 e^{-\lambda t}) e^{-(b+A_0 e^{-\lambda t})\tau} dt. \tag{A3}$$

Assuming that the background count rate is independent of time, this expression may be simplified via distribution to yield

$$M_{(t_1,t_0)}=\int_{t_0}^{t_1} be^{-(b+A_0e^{-\lambda t})\tau}dt+\int_{t_0}^{t_1}(A_0e^{-\lambda t})e^{-(b+A_0e^{-\lambda t})\tau}dt. \tag{A4}$$

The second term in this expression has a closed form solution.[11] As a result, Eq. (A4) may be further simplified

$$M_{(t_1,t_0)} = be^{-b\tau}\int_{t_0}^{t_1} e^{-(A_0e^{-\lambda t})\tau}dt + \frac{e^{-b\tau}}{\lambda\tau}\left(e^{-\left(A_0\tau e^{-\lambda t_1}\right)}-e^{-\left(A_0\tau e^{-\lambda t_0}\right)}\right). \tag{A5}$$

To derive an expression for the first term of Eq. (A5) first perform a change of variables of

$$y = A_0e^{-\lambda t}\tau.$$

The integral from the first term of Eq. (A5) can be represented as a function of y

$$\int_{t_0}^{t_1} e^{-(A_0e^{-\lambda t})\tau}dt = \frac{-1}{\lambda}\int_{y_0}^{y_1}\frac{e^{-y}}{y}dy, \tag{A6}$$

where $y_0 = A_0e^{-\lambda t_0}\tau$ and $y_1 = A_0e^{-\lambda t_1}\tau$.

Equation (A6) may be expanded via Taylor series[11] yielding

$$\frac{-1}{\lambda}\int_{y_0}^{y_1 1}\frac{e^{-y}}{y}dy = \frac{-1}{\lambda}\left[\ln\left(\frac{y_1}{y_0}\right)-(y_1-y_0)+\frac{y_1^2-y_0^2}{2\times 2!}-\frac{y_1^3-y_0^3}{3\times 3!}+\frac{y_1^4-y_0^4}{4\times 4!}+\ldots\right]. \tag{A7}$$

Substitution of y_0 and y_1 into Eq. (A7) and simplification results in

$$\frac{-1}{\lambda}\int_{y_0}^{y_1}\frac{e^{-y}}{y}dy = (t_1-t_0)-\frac{1}{\lambda}\left[-(A_0\tau)(e^{-\lambda t_1}-e^{-\lambda t_0}) +\frac{(A_0\tau)^2}{4}((e^{-\lambda t_1})^2-(e^{-\lambda t_0})^2) -\frac{(A_0\tau)^3}{18}((e^{-\lambda t_1})^3-(e^{-\lambda t_0})^3) +\frac{(A_0\tau)^4}{96}((e^{-\lambda t_1})^4-(e^{-\lambda t_0})^4)+\ldots\right]. \tag{A8}$$

Because t_1 and t_0 are at the most 16 min apart, the counting intervals are short relative to the half-life of the source and $\frac{e^{-\lambda t_1}}{e^{-\lambda t_0}}$ is ~3%. The following simplifications were made:

$$(e^{-\lambda t_1})^k-(e^{-\lambda t_0})^k = (e^{-\lambda t_1}-e^{-\lambda t_0})ke^{-(k-1)\lambda t_0'} \qquad k=2,3,4,\ldots, \tag{A9}$$

where

$$e^{-\lambda t_1}+e^{-\lambda t_0} = 2e^{-\frac{\lambda(t_1+t_0)}{2}} = 2e^{-\lambda t_0'}. \tag{A10}$$

Substituting Eq. (A9) into Eq. (A8) yields

$$\begin{aligned}\frac{-1}{\lambda}\int_{y_0}^{y_1}\frac{e^{-y}}{y}dy &= t_1-t_0-\frac{1}{\lambda}\left[-(A_0\tau)(e^{-\lambda t_1}-e^{-\lambda t_0}) +\frac{(A_0\tau)^2}{4}((e^{-\lambda t_1})^2-(e^{-\lambda t_0})^2) -\frac{(A_0\tau)^3}{18}((e^{-\lambda t_1})^3-(e^{-\lambda t_0})^3) +\frac{(A_0\tau)^4}{96}((e^{-\lambda t_1})^4-(e^{-\lambda t_0})^4)+\ldots\right]\\ &= t_1-t_0+\left(\frac{A_0\tau}{\lambda}\right)(e^{-\lambda t_1}-e^{-\lambda t_0}) -\frac{(A_0\tau)^2}{2\lambda}(e^{-\lambda t_1}-e^{-\lambda t_0})e^{-\lambda t_0'} +\frac{(A_0\tau)^3}{6\lambda}(e^{-\lambda t_1}-e^{-\lambda t_0})e^{-2\lambda t_0'} -\frac{(A_0\tau)^4}{24\lambda}(e^{-\lambda t_1}-e^{-\lambda t_0})e^{-3\lambda t_0'}+\ldots.\end{aligned} \tag{A11}$$

Equation (A11) may be substituted for the integral of the first term of Eq. (A5) resulting in

$$\begin{aligned}M_{(t_1,t_0)} &= \frac{e^{-b\tau}}{\lambda\tau}(e^{-(A_0\tau e^{-\lambda t_1})}-e^{-(A_0\tau e^{-\lambda t_0})})+be^{-b\tau}(t_1-t_0)\\ &+\frac{A_0\tau}{\lambda}be^{-b\tau}(e^{-\lambda t_1}-e^{-\lambda t_0})\left(1-\frac{A_0\tau}{2}e^{-\lambda t_0'} +\frac{(A_0\tau)^2}{6}e^{-2\lambda t_0'}-\frac{(A_0\tau)^3}{24}e^{-3\lambda t_0'}+\ldots.\right)\end{aligned}$$

The final expression for the counts observed during the counting interval from t_0 to t_1 accounting for radioactive decay and background count rate used in the counts method is given by

$$\begin{aligned}M_{(t_1,t_0)} &= \frac{e^{-b\tau}}{\lambda\tau}(e^{-(A_0\tau e^{-\lambda t_1})}-e^{-(A_0\tau e^{-\lambda t_0})})+be^{-b\tau}(t_1-t_0)\\ &+\frac{A_0\tau}{\lambda}be^{-b\tau}(e^{-\lambda t_1}-e^{-\lambda t_0})\left(1-\frac{A_0\tau}{2}e^{-\frac{\lambda(t_1+t_0)}{2}} +\frac{(A_0\tau)^2}{6}e^{-\lambda(t_1+t_0)}-\frac{(A_0\tau)^3}{24}e^{-\frac{3\lambda(t_1+t_0)}{2}}\right).\end{aligned} \tag{A12}$$

This series was observed to converge rapidly so additional terms beyond those shown in Eq. (A12) were not included for use in the counts method.

[a]Author to whom correspondence should be addressed. Electronic mail: skappadath@mdanderson.org; Telephone: 713-745-2835; Fax: 713-563-8842.

[1]"Nuclear medicine/PET accreditation program requirements," American College of Radiology (ACR), 2012 [available URL: http://www.acr.org/~/media/ACR/Documents/Accreditation/Nuclear%20Medicine%20PET/Requirements.pdf, accessed 11 Feb 2013].

[2]"Performance measurement of gamma cameras," NEMA Standards Publication No. NU1-2007, (National Electrical Manufacturers Association, Washington, DC, 2007).

[3]R. Adams, G. J. Hine, and C. D. Zimmerman, "Deadtime measurements in scintillation cameras under scatter conditions simulat-

ing quantitative nuclear cardiography," J. Nucl. Med. **19**, 538–544 (1978).
[4]American Association of Physicists in Medicine, "Scintillation camera acceptance testing and performance evaluation," AAPM Report No. 6 (AAPM, College Park, MD, 1980), see www.aapm.org.
[5]L. Ferrer, G. Delpon, A. Lisbona, and M. Bardies, "Dosimetric impact of correcting count losses due to deadtime in clinical radioimmunotherapy trials involving iodine-131 scintigraphy," Cancer Biother. Radiopharm. **18**, 117–124, (2003)
[6]M. L. Bartlett, M. Webb, S. Durrant, A. J. Morton, R. Allison, and D. J. Macfarlane, "Dosimetry and toxicity of Quadramet for bone marrow ablation in multiple myeloma and other haematological malignancies," Eur. J. Nucl. Med. **29**, 1470–1477 (2002).
[7]S. Cherry, J. Sorenson, and M. Phelps, *Physics in Nuclear Medicine* (Saunders, Philadelphia, PA, 2003), p. 179.
[8]R. Adams, "Suggested revision of NEMA standards," J. Nucl. Med. **25**, 814–816 (1984).
[9]J. M. Bland and D. G. Altman, "Statistical methods for assessing agreement between two methods of clinical measurement," Lancet **1**(8476), 307–310 (1987).
[10]S. C. Kappadath, W. D. Erwin, and R. E. Wendt III, "Observed inter-camera variability in clinically relevant performance characteristics for Siemens Symbia gamma cameras," J. Appl. Clin. Med. Phys. **7**(4), 74–80 (2006).
[11]*Standard Mathematical Tables*, 26th ed. (CRC, Boca Raton, FL, 1981), p. 330, entry #522.